Tectonophysics xxx (2009) xxx–xxx

Contents lists available at ScienceDirect

Tectonophysics

journal homepage: www.elsevier.com/locate/tecto

The northwestern margin of the Basin-and-Range Province, part 1: Reflection profiling of the moderate-angle (~30°) Surprise Valley Fault

Derek W. Lerch [a,1], Simon L. Klemperer [a,*], Anne E. Egger [b], Joseph P. Colgan [b,2], Elizabeth L. Miller [b]

[a] Department of Geophysics, Stanford University, Stanford, CA 94305-2215, United States
[b] Department of Geological and Environmental Sciences, Stanford University, Stanford, CA 94305-2115, United States

ARTICLE INFO

Article history:
Received 5 June 2008
Received in revised form 2 February 2009
Accepted 28 May 2009
Available online xxxx

Keywords:
Seismic reflection profiling
Low-angle normal faults
Basin-and-Range Province
Surprise Valley Fault

ABSTRACT

Seismic reflection profiling demonstrates that the active, significant-offset Surprise Valley Fault that marks the western boundary of the Basin-and-Range Province in northernmost California dips at a moderate angle, only ~30° to ~2 km depth. A nearby seismic refraction/wide-angle reflection profile, albeit of lower-resolution, shows the fault-plane remains approximately planar to at least 7 km depth. Variably-tilted volcanic strata of known ages within the Surprise Valley basin demonstrate that ≥7 km of normal slip occurred along the Surprise Valley Fault within the past 8–4 Myr at a time-averaged slip rate of ~1–2 mm/yr, and that the fault rotated from an initial dip of as much as 60° to its present dip of 30°. The rotation of this isolated fault was not accomplished by domino-style rotation as seen elsewhere in the Basin-and-Range province, but rather by flexural rift-shoulder uplift aided by mid-crustal flow.

1. Introduction

The tectonically active eastern and western boundaries of the northern Basin-and-Range Province are well studied, yet comparatively little is known about the more diffuse northern margin of the province (Fig. 1). In northwest Nevada this region marks the transition from Basin-and-Range extension to the relatively unextended high volcanic plateaus in Nevada and northeastern California and southern Oregon (Fig. 1, inset). At this latitude, the westernmost significant-offset normal fault is the Surprise Valley Fault (SVF), an east-dipping fault developed along the eastern flank of the Warner Range that bounds Surprise Valley (Figs. 1 and 2; Duffield and McKee, 1986). Surprise Valley and the Warner Range are separated from the main part of the northwest Basin-and-Range province by ~90 km of unextended volcanic plateaus to the south and east, and thus offer an unusual opportunity to study the structural evolution of a significant-offset normal fault in relative isolation from other such structures (Fig. 1).

In this paper, we present the results of a 16-km long 2-D seismic reflection profile across Surprise Valley (Fig. 2) at the southern end of the Lake City segment of the SVF. The Lake City segment of the SVF steps east to the Cedarville fault segment and a topographic high or bulge occurs at the complex juncture and zone of overlap between these two fault segments (Fig. 1). Our reflection data image the SVF and its associated basin to a depth of ~2 km (Fig. 2). These vibroseis reflection data were collected to augment a ~300-km long explosive-source seismic refraction survey across the northwestern Basin-and-Range transition zone (Lerch et al., 2007) that separately imaged reflections from the fault plane of the Cedarville segment of the SVF to a depth of ~7 km (Fig. 3). A companion paper (Egger et al., in press) provides gravity and magnetic-field analysis along the reflection profile discussed here, giving additional insight into the nature of the Surprise Valley Fault and associated intra-basin structures.

Based on our data, the SVF appears comparable to other well-studied Basin-and-Range normal faults where originally steep fault planes have rotated to shallower angles during progressive fault slip, with concomitant rotation of foot-wall and hanging-wall rocks. The isolation of the SVF from other normal faults, however, makes it distinct from the planar, rotational domino-style faulting common in the Basin and Range (e.g. Proffett, 1977; Surpless et al., 2002). Instead, both foot-wall and hanging-wall dips flatten progressively away from the SVF, a smaller-scale example of the well-documented upturned flanks of rifted plateaus (Fig. 2A, e.g., Ebinger et al., 1999). Our reflection data augment the extensive datasets that address the still controversial and highly-debated mechanics of normal faulting (see Axen, 2007 for a recent review) by demonstrating that despite being isolated from other large normal faults, the SVF began its history as a high-angle normal fault, and progressively rotated to shallower dips while maintaining its planar geometry in the upper crust.

Our new dataset also adds to the still small suite of reflection images of shallow-to-moderate angle faults that have been seismically

* Corresponding author.
E-mail address: sklemp@stanford.edu (S.L. Klemperer).
[1] Now at: Department of Environmental Studies, Feather River College, Quincy, CA 95971, United States.
[2] Now at: U.S. Geological Survey, 345 Middlefield Road, Menlo Park CA 94025, United States.

0040-1951/$ – see front matter © 2009 Elsevier B.V. All rights reserved.
doi:10.1016/j.tecto.2009.05.028

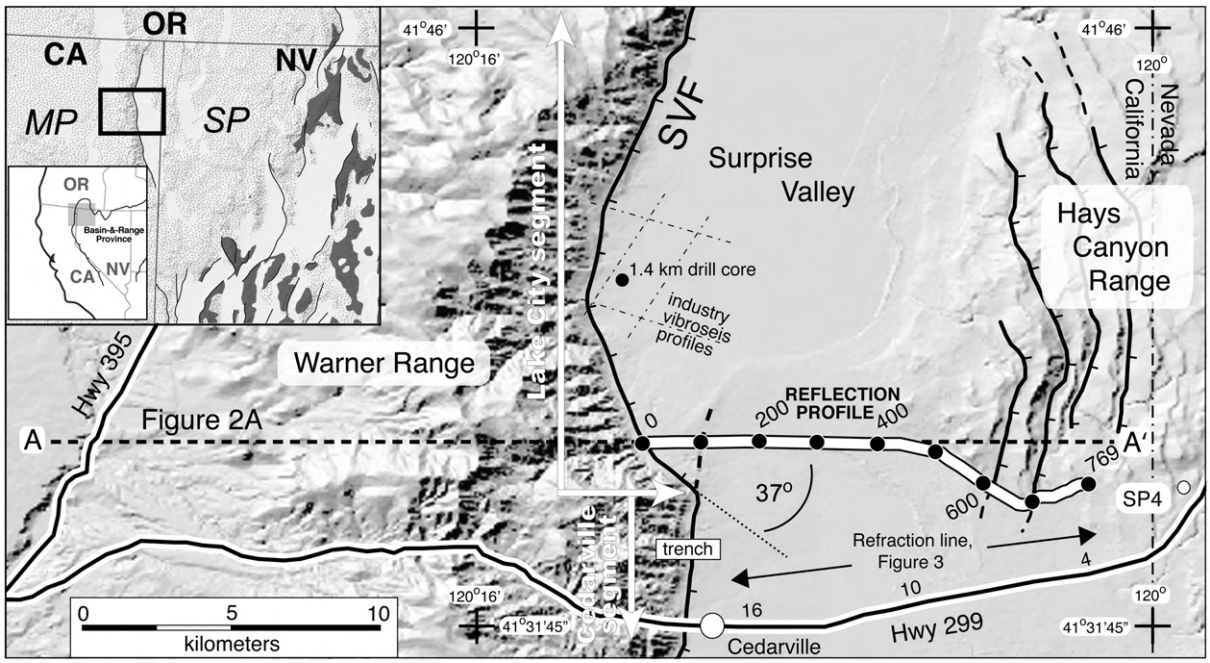

Fig. 1. Shaded relief map of Surprise Valley and the Warner Range in northeastern California. Location of reflection profile is shown by wide white line approximately 5 km north of the 2004 Stanford refraction line (Lerch et al., 2007) that ran along California State Highway 299. Distances along line are given by common midpoint (CMP) locations spaced at 20 m. East-dipping Surprise Valley Fault (SVF) is shown by solid black line with barbs on the hanging-wall block. Exploratory geothermal drill core (Miller et al., 2005) is ~6 km north of our profile. SP4: Shotpoint 4 from the 2004 Stanford refraction line. Line A–A′: location of geologic cross-section (Fig. 2A). Angle of intersection between our reflection profile and the SVF is ~37°. White rectangle across the SVF mid-way between Cedarville and our reflection profile marks the USGS trenching project (Personius et al., 2007). Dash–dot lines mark location of commercial vibroseis velocity profiles (Benoit, 2004). Numbers along Highway 299 are receiver offsets (km) shown in Fig. 3. Inset map shows simplified geologic setting and boundaries of Basin-and-Range Province. Dark gray regions: Paleozoic and Mesozoic igneous and metamorphic rocks. Stippled regions: Tertiary volcanic rocks. Light gray regions: Quaternary deposits. MP and SP mark the Modoc and Sheldon volcanic plateaus that surround Surprise Valley.

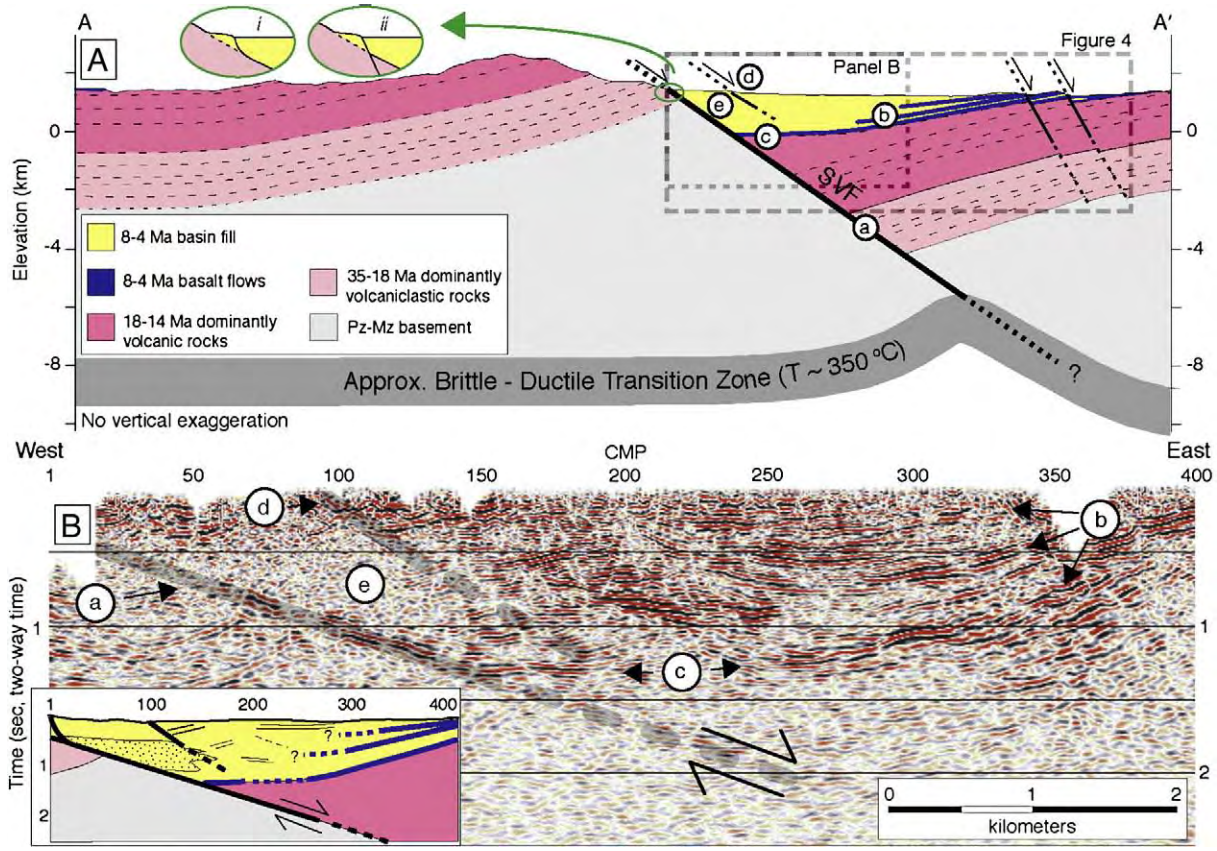

Fig. 2. Geologic and seismic cross-sections of Surprise Valley along line A–A′ (Fig. 1). Fig. 2A: regional cross-section based on field mapping, well-control, and seismic profile (Fig. 2B) after correction for the obliquity of profile to fault dip direction. Note progressive thickening of the young (8–4 Ma) volcanic section in the hanging wall near the SVF. Inset ellipses illustrate possible near-surface geometries for the SVF, described in text. Fig. 2B: 2-D time migrated image of the Surprise Valley basin. Annotated features described further in the text: a: SVF fault-plane reflection; b: possible intra-basin basalt flows; c: shallower dips at base of section; d: strata offset by minor normal fault; and e: transparent zone, probably coarse alluvium. Inset diagram: line drawing of significant features of seismic section. Seismic section displayed with no vertical exaggeration based on seismic wavespeed for the basin fill of 2 km/s.

Please cite this article as: Lerch, D.W., et al., The northwestern margin of the Basin-and-Range Province, part 1: Reflection profiling of the moderate-angle (~30°) Surprise Valley Fault, Tectonophysics (2009), doi:10.1016/j.tecto.2009.05.028

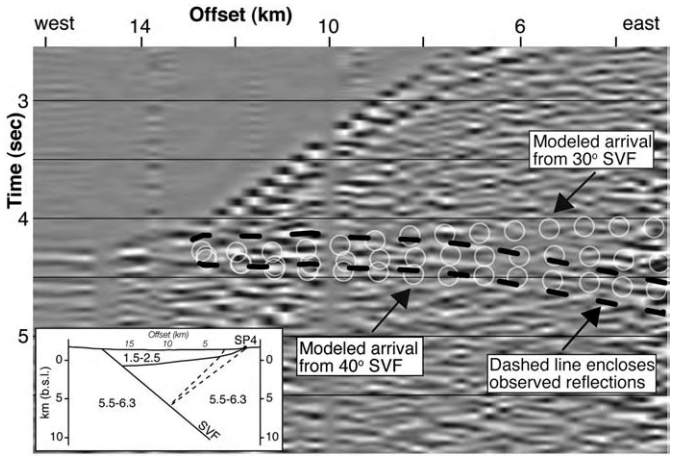

Fig. 3. Shot-gather from Shotpoint 4 (see Fig. 1), approximately 5 km south of reflection profile in Fig. 2. Trace and receiver spacing is ~600 m. Shot-gather (no move-out applied) shows first arrivals across Surprise Valley, and reflection from the SVF with reverse move-out (i.e., reflection on long-offset traces arrives earlier than the same reflection on near-offset traces) delineated by region enclosed by dashed black line. Superimposed on the explosive-source data are modeled arrivals corresponding to varying dip geometries of the SVF using the velocity model from the 2004 Stanford refraction line (Lerch et al., 2007) while holding all else unchanged. Thin gray circles illustrate modeled arrivals from the SVF that arrive earlier and later than the observed phase, corresponding to modeled fault geometries dipping 30°, 35° and 40°. The shallowest part of the fault-plane reflection recorded at offsets 13–10 km best fits a 30° dip, whereas the deepest parts of the fault-plane reflection recorded at offsets 6–3 km best fits a 40° dip. Schematic velocity model used in modeling is shown in inset, velocities are given in km/s, depths given in km below sea level (no V.E.). Dashed line on inset shows approximate raypath for reflected energy observed at 3 km offset, sampling the SVF at a depth of ~7 km below the surface. Because of strong raypath bending (refraction) at the basin–basement interface, the fault-plane reflection appears to merge with the first arrival almost vertically above the deepest point in the basin, rather than at the surface trace of the fault as would be predicted for a constant-wavespeed halfspace.

active from the late Quaternary to present. Goodliffe and Taylor (2007) image the Moresby Fault, Woodlark Basin, dipping ≥29° to about 7 km depth below sea floor, and Sachpazi et al. (2003) a possible low-angle detachment beneath the Gulf of Corinth to >5 km dipping <30° in the earthquake slip direction. Within the Basin-and-Range Province, Abbott et al. (2001) imaged the Dixie Valley Fault to 500 m depth, and inferred that its 25–30° dip continued to at least 2 km depth, and Johnson and Loy (1992) imaged the Santa Rita fault dipping 20° to nearly 6 km beneath the Tucson Basin. In this paper we show fault-plane reflections from the Surprise Valley Fault to about 7 km depth. All these areas (except Gulf of Corinth) have high heat flow and active hot springs. Dixie Valley hosts a geothermal system and associated power plant, and Surprise Valley is the site of exploratory geothermal drilling (e.g. Benoit, 2004; Kennedy and van Soest, 2006). These conditions of high heat flow (hence a thin brittle upper crust) and active fluid systems (with potential for fluid over-pressuring) may be enabling factors for seismic rupture on shallow-to-moderate angle faults.

2. Geologic setting

The Surprise Valley Fault has a map geometry typical of Basin-and-Range style normal faults, trending north–south with distinct arcuate segments (Fig. 1). The rocks of the Warner Range, the footwall of the SVF, comprise a ≥3 km-thick sequence of Oligocene and Miocene volcanic, volcaniclastic and sedimentary units that dip 15–25° W (Fig. 2A), (Duffield and McKee, 1986; Fosdick et al., 2005; Miller et al., 2005). Detailed mapping of the volcanic units suggests there is likely an unconformity between 33–26 Ma Oligocene calc-alkaline units and 17–14 Ma basalts and basaltic andesites (Duffield and McKee, 1986; Carmichael et al., 2006). The youngest tilted units in this sequence are ~14 Ma basalt flows with a maximum dip of 15° to the west, exposed along the crest of the southern part of the range (Duffield and McKee, 1986). In the vicinity of the reflection profile, however, no Mid-Miocene rocks are present: ages in the volcanic units at the crest of the range are 26 Ma (J.P. Colgan, unpublished data; Duffield and McKee, 1986).

Late Miocene to Pliocene (8–4 Ma) basalt flows and tuffaceous sediments exposed on the east side of Surprise Valley are similar in composition and age to flat-lying volcanic units west of the Warner Range (Fig. 2A), leading Carmichael et al. (2006) to suggest that these younger volcanic rocks provide a maximum age for initiation of faulting along the SVF. However, these 8–4 Ma rocks are not present at high elevations within the range itself, leaving open the possibility that significant topography already existed by the time they were deposited. Thermochronologic data from the base of the exposed Cenozoic section approximately 20 km south of our seismic profile are inferred to record two phases of slip on the SVF: an earlier period of slip commencing around 14 Ma and continuing to 8 Ma, and a distinct younger phase beginning about 3–4 Ma (Colgan et al., 2008a).

The poorly consolidated volcaniclastic footwall rocks of the SVF have preserved few unambiguous, measurable fault surfaces, thus precluding direct measurement of the dip of the SVF. Although steeply dipping Quaternary faults are exposed in gravel pits (Hedel, 1984) and have been trenched within the lacustrine sediments of pluvial Lake Surprise (Personius et al., 2007), their relationship to the range-bounding fault that we have imaged in the subsurface is not known.

Presently, Surprise Valley hosts three lakes, the Upper, Middle, and Lower Lakes, separated by minor topographic highs and significant westward steps in the rangefront, reflecting the large-scale segmentation of the SVF. Our reflection profile crosses the south end of the Lake City segment of the fault, close to the boundary with the Cedarville segment of the fault (Fig. 1). Our profile highlights the structural complications inherent in these boundary zones, described here and in more detail in Egger et al. (in press), but also lends important insight into the evolution of the Surprise Valley Fault system and the valley itself.

3. Data acquisition and processing

In September 2004, we completed a ~300 km explosive-source seismic refraction survey across the northwestern Basin-and-Range transition zone (Lerch et al., 2007), with a ~60 km teleseismic deployment embedded within the active-source profile to provide complementary crustal structure information (Gashawbeza et al., 2008). These data were augmented by vibroseis profiling using the 29,090 kg (64,000 lb) Network for Earthquake Engineering Simulation (NEES)-UT-Austin T-Rex tri-axial (P- and S-wave) vibrator in two separate reflection profiles, the 16 km basin-imaging line discussed here, and a ~40 km crustal-scale line across the Black Rock Desert and Black Rock Range (Lerch et al., 2008).

Our 2-D basin-imaging reflection profile is approximately orthogonal to the overall trend of the SVF, crossing Surprise Valley ~5 km north of Cedarville, CA (Fig. 1). Our vibrator could not be used on paved roads, because of the large teeth on the shear-wave base-plate (Lerch et al., 2008), hence our choice of route shown in Fig. 1, despite the less-than-favorable geometry with an oblique crossing of our profile over the SVF. Access limitations prevented profiling west of the surface trace of the SVF along this profile (westernmost receiver location and vibration point were respectively 160 m west and 80 m east of the geomorphic expression of the fault trace at CMP 0). Coupled with some instrument failure in the field, no reflection data were acquired imaging the SVF shallower than 0.5 s (Fig. 2B). Over 4 days, we generated a total of 1600 individual 60 sec sweeps at 10 m intervals along the 16 km profile, combined during processing into 40 m source arrays. These sweeps were recorded at a 4 ms sample rate

Please cite this article as: Lerch, D.W., et al., The northwestern margin of the Basin-and-Range Province, part 1: Reflection profiling of the moderate-angle (~30°) Surprise Valley Fault, Tectonophysics (2009), doi:10.1016/j.tecto.2009.05.028

by RefTek 125A seismographs (Texans) with 4.5 Hz geophones spaced every 40 m. The source effort per line-kilometer was chosen to be comparable to other successful single-vibrator upper-crustal surveys (e.g., Belcher et al., 1986) for this first test of the NEES vibrator in a continuous profiling application.

We used linear up-sweeps that were dominantly 5–80 Hz (4 octaves), nearly all of which were P-wave (limited testing of S-wave sweeps was aborted due to mechanical problems). Full details of cost-effective experimental design to efficiently manage vibroseis recording utilizing PASSCAL Texans that have only limited recording memory are given in Lerch et al. (2008).

Data were pre-processed by PASSCAL and are archived at the IRIS Data Management Center (DMC). Our 20-m common midpoint (CMP) data (40-m source arrays, 40-m receiver spacing) were processed using ProMAX seismic software, sequentially consisting of amplitude-balancing (500 ms AGC), frequency filtering (10-14-36-42 Hz band-pass), velocity analysis, predictive deconvolution (160 ms operator length, 10 ms prediction distance, 0.1% pre-whitening), CMP stacking, and post-stack time migration.

4. Basin structure

On our seismic data, we recognize an east-dipping reflection from the SVF (Fig. 2B, reflection a), but the brightest reflections are within the basin, 0 to 1.5 s from CMP 200 to 400 (Fig. 2B, reflections b), and have a low average wavespeed of 2.0 ± 0.2 km/s constrained by our reflection semblance analysis (e.g. Yilmaz, 2001) and by velocity modeling of our crustal-scale refraction study (see Fig. 7 of Lerch et al., 2007). West-dipping reflections continue east to the western edge of Hays Canyon Range (Fig. 4, ~0.5 s at CMP 700), but show no resolvable offsets even though our line crosses several minor east-dipping normal faults (Figs. 1, 2A) that are individually responsible for <500 m of vertical displacement and cut the late Miocene to Pliocene volcanic section (Egger et al., in press). The stratigraphically deepest west-dipping reflections at 2.0 s, CMP 480, and possibly 2.1 s, CMP 520 (Fig. 4) would project to intersect the projection of the SVF reflection at 2.5–3.0 s, at 3.5–4.0 km depth. Ray-trace modeling of direct and refracted arrivals (Egger et al., in press, their Fig. 6) shows that seismic wavespeeds increase with depth, presumably due to compaction as well as to facies changes, but our recorded refracted arrivals are confined to the upper 1.5 km of the basin so the total depth of the basin remains uncertain.

The brightest reflections in the basin may correspond to thin basalt flows, typically 2–5 m thick where drilled in boreholes and exposed near the east end of the profile, within seismically reflective lacustrine strata, tuffs and tuffaceous sediments. Source gathers acquired in the reflection experiment show first-arrival refraction patterns consistent with thin, high-velocity layers, too thin to separately model, embedded in the overall low-velocity basin fill. The deepest of the bright reflections (Fig. 2B, b) likely represent the youngest dated basalt flows exposed to the east (~4 Ma, Carmichael et al., 2006), and the shallower reflections even younger flows. The age range of these units temporally overlaps with at least some of the slip along the SVF (Duffield and McKee, 1986; Colgan et al., 2006, 2008b). Dips of these reflectors shallow up-section, from ~15° for the deepest reflections, to ~10° for the shallowest (calculated for an average seismic wavespeed of 2 km/s). Accounting for the likely wavespeed increase with depth would further accentuate the progressive steepening of these flows with depth and age. This increasing dip with depth is compatible with our interpretation of a growth fault relationship such that volcanic flow units have shallower dips up-section. Where exposed on the eastern side of Surprise Valley, these units dip more shallowly than Mid-Miocene units to the south and Oligocene units present in Warner Range at this latitude (10° vs. 15–25°), consistent with slip on the SVF prior to their eruption at 8 Ma, but subsequent to the youngest (~14 Ma) units exposed in the footwall block in the Warner Range (e.g. Colgan et al., 2008a).

The reflection interpreted as the deepest west-dipping basalt flows (Fig. 2B, reflection c) is discontinuous near CMP 230, and appears to shallow and truncate against the SVF at 1.4 seconds. This may be related to normal drag on the fault, or to some combination of initial dip related to pre-existing relief within the Surprise Valley basin, and/or smaller offset faults within the basin fill itself (aligned offsets d; also see Egger et al., in press).

By projecting the late Miocene to Pliocene volcanic flows exposed along the west side of the Warner Range to their intersection with the projection of the SVF, a minimum slip of at least 7 km since their eruption at 8–4 Ma is implied (Fig. 2A). The total magnitude of slip is at least ~10 km based on the hanging-wall projection of the Cretaceous–Tertiary unconformity (light pink-grey contact in Fig. 2A), so several km of slip likely predates the eruption of the 8 Ma basalts. These projections imply slip rates of 1–2 mm/yr, similar to modern rates suggested by Quaternary fault scarps and preliminary paleo-seismic results from the SVF (de Polo and Anderson, 2000; Personius et al., 2007).

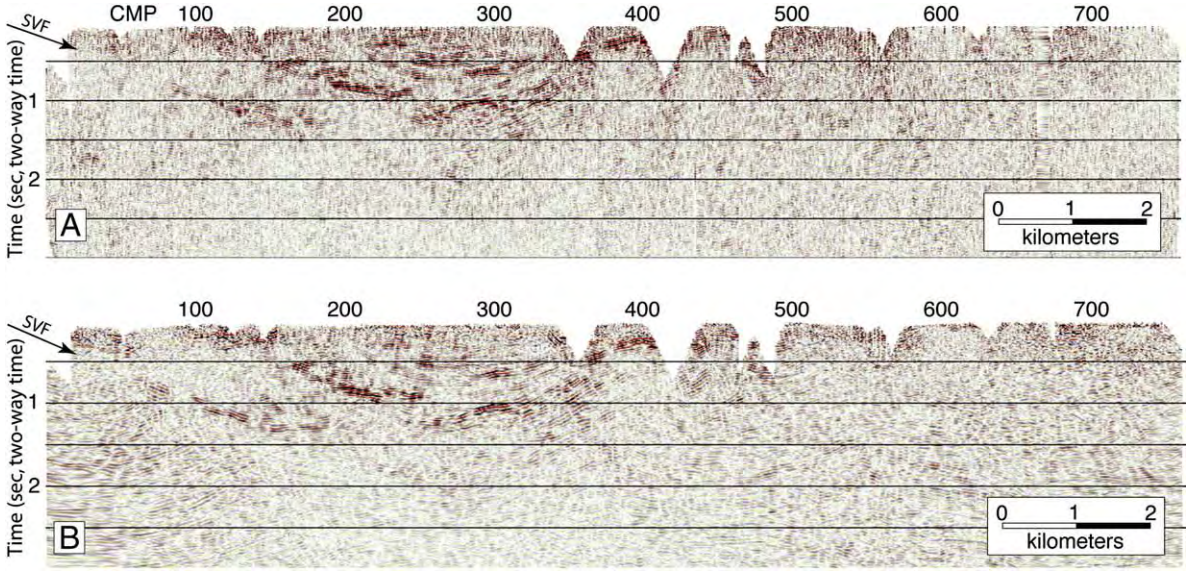

Fig. 4. Complete reflection section from Surprise Valley. Panel A is the unmigrated CMP stack. Post-stack time migration applied in Panel B.

Please cite this article as: Lerch, D.W., et al., The northwestern margin of the Basin-and-Range Province, part 1: Reflection profiling of the moderate-angle (~30°) Surprise Valley Fault, Tectonophysics (2009), doi:10.1016/j.tecto.2009.05.028

Several reflections with variable dips in the central portion of the Surprise Valley basin (CMP 150–250), the strongest of which are shown in the simplified line drawing (Fig. 2B, inset), are difficult to interpret. These variable dips may be attributed to two likely sources: a complex basin development history with volcanic flows, alluvial and colluvial sedimentation, and fluctuating lake levels (e.g., Reheis et al., 2002); and overpressured, strongly reflective, basin strata related to the geothermal potential of the area as evidenced by surface hot springs and mud volcanoes (e.g., McLeod, 1951; Bezore, 1984), all cut by minor intra-basin faults (Egger et al., in press).

We interpret the transparent region near the SVF (CMPs 50–150, ≤1 s) to be coarse alluvium shed from the Warner Range during basin subsidence (Fig. 2B, zone e), similar to other reflection profiles across large-offset normal faults in the Basin-and-Range Province (e.g., Gans et al., 1985; Okaya and Thompson, 1985). This alluvium is bound on the west by the SVF, and on the east by reflection packages that disappear against and interfinger with the abrupt facies change represented by the reflection-free fan deposits. Egger et al. (in press) find that seismic wavespeeds are higher in this transparent zone e than in the reflective lacustrine facies further east, though velocities are not well-determined due to poor ray geometry and limited ray penetration. The similar non-reflective, inferred alluvial-fan facies above the fault tip of the Dixie Valley fault in central Nevada (Okaya and Thompson, 1985) is there shown from refraction data to have a seismic wavespeed of 2.3–2.6 km/s in contrast to the typical valley-fill wavespeed of 2.1 km/s (Thompson et al., 1967).

The most tectonically significant reflections on our seismic section are from the SVF that provides the structural control for the evolution of the Surprise Valley basin and the uplift of the Warner Range (Fig. 2B, reflection a), visibly truncating intra-basin reflections. The image of the SVF in Fig. 2B dips 18° when migrated and displayed at a wavespeed of 2.0 km/s appropriate for the reflective section of basin fill. Poor reflectivity at the west end of the profile (west of c. CMP 100) limits our velocity resolution from semblance analysis. If the average seismic velocity is faster in the non-reflective, coarser alluvial-fan sequence close to the fault tip than in the reflective lacustrine facies in the main depocenter, then the fault might be slightly listric, steepening towards the surface. To provide conservative (steep) estimates of fault dip, we use a range of average velocities down to the fault of 2.4 ± 0.4 km/s, leading to apparent dips of $22 \pm 4°$ along the line of profile. This is only an apparent dip, because our 2-D profile has an oblique ($37 \pm 3°$) intersection with the strike of the SVF at the western end of the survey (Fig. 1). Correcting for the apparent dip created by this geometry and associated side-swipe (e.g., Slotnick, 1959) implies a true dip of the fault plane of $28 \pm 6°$ (a 22° dip would correspond to a fault obliquity of 34° and average seismic wavespeed of 2.0 km/s; a 34° dip is calculated for a fault obliquity of 40° and average seismic wavespeed of 2.8 km/s).

This corrected dip ($28 \pm 6°$) represents the true dip of the fault plane at this location, though the dip in the slip direction is likely lower. The actual slip sense on this $037 \pm 3°$-trending fault tip would contain a dextral component if the hanging-wall motion complies (as is required to avoid significant space problems) with the 090° regional slip direction (top to the east), suggesting a fault dip in the slip direction of $22 \pm 4°$, consistent with the lowest dips observed for the rupture planes of active continental normal faults (Johnson and Loy, 1992; Collettini and Sibson, 2001).

Oligocene volcanic strata preserved in the Warner Range dip $20 \pm 5°$ to the west as a result of footwall-block rotation during slip on the SVF (Fosdick et al., 2005). Restoring this rotation of the footwall units results in an initial fault dip of ~37–59°, compatible with experimentally-derived normal-fault formation geometries of 54–69° (for Berea sandstone, Twiss and Moores, 1992) and with the standard high-angle model (~60°) for the upper-crustal rupture of Basin-and-Range normal faults (e.g., Friedrich et al., 2004; Personius and Mahan, 2005).

Two additional datasets north and south of our reflection profile confirm that the SVF dips 30–40° for at least 12 km along strike, and in two adjacent segments. Four commercial vibroseis profiles 6 km north of our reflection profile (Fig. 1), still within the Lake City segment of SVF, provide velocity information that suggests the basin–basement interface (presumably the SVF) dips ~30° (Benoit, 2004). The 2004 Stanford refraction profile 6 km south of our reflection profile, across the Cedarville segment of the SVF (Fig. 1), shows a reflection from Shotpoint 4 with reverse move-out (far-offset arrivals arrive earlier than near-offset arrivals), the signature of a reflector dipping steeply back towards the shotpoint, that is best matched by a fault that dips ~30–40° to at least 7 km depth (Fig. 3).

A splay from the main fault strand of the Cedarville segment crosses our survey-line just east of the SVF and produces a topographic bench, accommodating at least minor offset near CMP 100 (Fig. 1). We interpret the western terminations of a thin sequence of west-dipping reflectors (10°–15°) near CMP 100 to be basin strata offset by this fault (Fig. 2B, alignment d). This fault splay dips $34 \pm 4°$ after migration at seismic wavespeeds of 2.1 ± 0.2 km/s (we use lower velocities than for migrating the SVF because this fault splay is shallower and more distal from the alluvial fan). The minor fault splay (d on Fig. 2B) appears steeper than the dip of the SVF (a on Fig. 2B) largely because the minor fault trends north–south, so the reflection points (d on Fig. 2B) are vertically beneath the west–east seismic profile (apparent dip is true dip in this case), in contrast to the reflection points from the SVF that are displaced south of the profile due to local obliquity of the SVF to the seismic profile. The appearance on Fig. 2B that the splay fault (e) will intersect the SVF reflection (a) at ~2 s travel time is thus largely an artifact of the 3D geometry. Within our uncertainties the minor fault ($34 \pm 4°$) could either be parallel to the SVF ($26 \pm 8°$) along the line of section AA′ (Fig. 2A), or could sole into the SVF (inset to Fig. 2B).

5. Discussion

Our data described above highlight the complexity of the detailed geometry of major continental normal faults, even when formed in near isolation from other parallel faults. The SVF formed at a high-angle (~50–60°), then rotated to its shallow present-day dip of ~30°, while accommodating at least 10 km of dip-slip motion over the last 14 Ma. Although upper-crustal units undergo progressive flexure in the foot-wall and hanging-wall blocks as they approach the SVF, the fault plane itself remains fairly planar to ≥7 km depth (Fig. 3) and its development appears indistinguishable from the upper-crustal evolution of domino-style normal faults elsewhere in the Basin and Range (e.g., Proffett, 1977; Chamberlin, 1983; Gans et al., 1985).

Its isolation from other significant structures, however, makes the SVF unusual within the Basin and Range, affording an opportunity to observe the development of a normal fault in continental crust under relatively simple boundary conditions. The SVF is responsible for the tilting observed in the Warner Range and in Surprise Valley, but this tilting is not a function of domino-style normal faulting and block rotation (e.g. Proffett, 1977). The tilting observed in the Warner Range is a smaller-scale example of that seen along rift-bounded plateaus where flat-lying stratigraphy rises topographically toward the bounding rift, as observed along the East African Rift and the Red Sea (see Fig. 1 of Ebinger et al., 1999). This tilting was explained by Heiskanen and Vening Meinesz (1958) as due to the isostatic uplift of a horst footwall after removal of the load of the hanging-wall graben. The ~15 km basin width of Surprise Valley is comparable to the Dobe and Addo-Do extensional basins in Afar where elastic thicknesses are constrained to be between 5 and 10 km (Hayward and Ebinger, 1996; Foster and Jackson, 1998). The radius of curvature of tilted volcanic strata in our footwall block (the Warner Range) (Fig. 2A) is approximately 65–70 km, compatible with forward modeling of plateau-bounding rifts by Ebinger et al. (1999) in which an elastic

Please cite this article as: Lerch, D.W., et al., The northwestern margin of the Basin-and-Range Province, part 1: Reflection profiling of the moderate-angle (~30°) Surprise Valley Fault, Tectonophysics (2009), doi:10.1016/j.tecto.2009.05.028

thickness of 10 km produced a surface with a radius of curvature of ~60 km. Given the high heat flow (≥100 mW/m^2) and low surface conductivities (~2 W/m/K; hence, near-surface temperature gradient of 50 °C/km) of the Surprise Valley region (Blackwell et al., 1991; Benoit, 2004), we expect the brittle–ductile transition zone, and thus the deeper limit of effective elastic thickness, to lie at less than 9 km depth (Fig. 2A). Modeling by Buck (1993) indicates that only in cases of very low elastic thickness (<10 km) will isolated normal faults bend and rotate to shallow angles before being replaced by younger, high-angle faults. The brittle–ductile transition zone beneath Surprise Valley should be slightly perturbed by motion along the SVF (Fig. 2A), but conductive cooling should re-establish it at ~9 km depth at a characteristic time-scale of ~2.5 Ma (e.g., Turcotte and Schubert, 1982). Thus the 350 °C isotherm (our proxy for the brittle–ductile transition zone) should be elevated by less ≤3 km, being the amount of vertical motion along the SVF since 2.5 Ma for ≤5 km dip-slip (Fig. 2A). The absence of any observable Moho relief beneath the SVF (see Fig. 7 of Lerch et al., 2007) corroborates our supposition of low elastic thickness and indicates that crustal flow in the middle to lower crust must compensate for the fault rotation.

Paleoseismic studies constrain the surface dip of the most youthful fault scarps along the Cedarville segment of the SVF to be ~65–70° (Personius et al., 2007), far too steep to be the main fault plane imaged in our profile (even with the most extreme assumptions about high seismic velocity and large obliquity between fault dip and profile trend) and also too steep to account for the ~15–25° tilt of Cenozoic strata in the Warner Range. We recognize two likely explanations for this discrepancy, aside from the separation of the trench from the profile (the trench is 3 km south of the reflection line, across a different segment of the fault). First, that slip on the modern SVF (measured in the trench) roots into the lower-angle SVF at depth (Fig. 2A, inset ellipse i), or second, that the active trace of the SVF is a young feature in the Surprise Valley–Warner Range system, cutting and offsetting the shallower SVF which is now unfavorably oriented for slip (Fig. 2A, inset ellipse ii) (cf. Proffett, 1977; Chamberlin, 1983).

Despite our inability to resolve the above discrepancy (at least until the next large earthquake on the SVF), multiple datasets indicate that the SVF represents an active Basin-and-Range normal-fault system. In addition to seismic, thermochronologic, and geologic data, geodetic strain measurements of present-day deformation show a strong velocity gradient across the Surprise Valley–Warner Range system (Hammond and Thatcher, 2005). From east to west, across the Sheldon Plateau–Surprise Valley transition, velocity vectors shift from NW-directed to NNW-directed and increase in velocity from approximately 3 mm/yr to 5–7 mm/yr (relative to stable North America). At face value, these geodetic velocities taken together with the N–S trend of the SVF suggest that the modern fault system should include a dextral strike-slip component. More detailed studies are in progress to determine along what faults these motion(s) are taking place. This strike-slip motion may be loosely linked to the temporal northwestward growth of the Eastern California Shear Zone–Walker Lane Fault Zone system (e.g., Oldow, 2003; Faulds et al., 2005). However, it is clear from the map-scale corrugated morphology of the SVF that the SVF has accommodated very little strike-slip motion in its history of slip; and indeed, the sense of offset of the SVF between adjacent fault segments would be more consistent with sinistral than dextral motion (Egger et al., in press). This may indicate that the 1–2 mm/yr component of strike-slip motion inferred from geodetic measurements is very young, or is being accommodated along as yet unmapped faults within Surprise Valley.

Acknowledgments

Numerous hard-working volunteers made this experiment possible, as well as the Modoc County Road Department (Tom Minto and John Wistos), the Cedarville Fairgrounds (Tracy Green), and the UT-Austin T-Rex administrators and operators (Ken Stokoe, Farn-Yuh Menq, and Cecil Hoffpauir). Support for vibroseis profiling was provided by NSF-Geoenvironmental Engineering and Geohazard Mitigation grant 0444696; principal funding for the explosive-source profiling was provided by NSF-Earthscope grant 0346245 and by the Petroleum Research Fund of the American Chemical Society grant 39063-AC8; geologic fieldwork was supported by NSF grant EAR-0229854. Field support and instruments were provided by the PASSCAL Instrument Center, and ProMAX reflection processing software by a Landmark academic grant. Data are archived at, and available from, the IRIS Data Management Center. Thorough, constructive reviews by G. Axen, P. Cashman and one anonymous reviewer improved both the scientific content and clarity of this paper.

References

Abbott, R.E., Louie, J.N., Caskey, S.J., Pullammanappallil, S., 2001. Geophysical confirmation of low-angle normal slip on the historically active Dixie Valley fault, Nevada. Journal of Geophysical Research 106, 4169–4181.

Axen, G.J., 2007. Research focus: significance of large-displacement, low-angle normal faults. Geology 35, 287–288.

Belcher, S.W., Pratt, T.L., Costain, J.K., Coruh, C., 1986. Alternative processing techniques and data improvement provided by single-sweep recording. Geophysics 51, 1736–1742.

Benoit, D., 2004. Exploration of the Lake City geothermal system and flow testing of the Phipps 2 well. GRED Report DE-SCO4-02LA67912. U.S. Department of Energy.

Bezore, S.P., 1984. New technical map; geothermal resources of California. California Geology 37, 115–118.

Blackwell, D.D., Steele, J.L., Carter, L.S., 1991. Heat-flow patterns of the North American continent; a discussion of the geothermal map of North America. In: Slemmons, D.B., Engdahl, E.R., Zoback, M.D., Blackwell, D.D. (Eds.), Neotectonics of North America. In: Decade of North American Geology. Geological Society of America, Boulder, CO, pp. 423–436.

Buck, W.R., 1993. Effect of lithospheric thickness on the formation of high- and low-angle normal faults. Geology 21, 933–936.

Carmichael, I.S., Lange, R.A., Hall, C.M., Renne, P.R., 2006. Faulted and tilted Pliocene olivine–tholeiite lavas near Alturas, NE California, and their bearing on the uplift of the Warner Range. Geological Society of America Bulletin 118, 1196–1211.

Chamberlin, R.M., 1983. Cenozoic domino-style crustal extension in the Lemitar Mountains, New Mexico: a summary. In: Chapin, C.E., Callender, J.F. (Eds.), Guidebook, 34th Field Conference, Socorro Region II, vol. 34. New Mexico Geological Society, Socorro, New Mexico, pp. 111–118.

Colgan, J.P., Dumitru, T.A., Miller, E.L., Reiners, P.R., 2006. Cenozoic tectonic evolution of the Basin and Range Province in northwestern Nevada. American Journal of Science 306, 616–654.

Colgan, J.P., Shuster, D.L., Reiners, P.W., 2008a. Two-phase Neogene extension in the northwestern Basin and Range recorded in a single thermochronology sample. Geology 36, 631–634. doi:10.1130/G24897A.1.

Colgan, J.P., Egger, A.E., John, D.A., 2008b. Oligocene and Miocene arc volcanism in northeastern California. EOS, Transactions — American Geophysical Union 89 (53) (V31B-2131).

Collettini, C., Sibson, R.H., 2001. Normal faults, normal friction? Geology 29, 927–930.

de Polo, C.M., Anderson, J.G., 2000. Estimating the slip rates of normal faults in the Great Basin, USA. Basin Research 12, 227–240.

Duffield, W.A., McKee, E.H., 1986. Geochronology, structure, and basin–range tectonism of the Warner Range, northeastern California. Geological Society of America Bulletin 97, 142–146.

Ebinger, C.J., Jackson, J.A., Foster, A.N., Hayward, N.J., 1999. Extensional basin geometry and the elastic lithosphere. Philosophical Transactions of the Royal Society of London A357, 741–765.

Egger, A.E., Glen, J.M.G., Ponce, D.A., in press. The northwestern margin of the Basin and Range Province, part 2: structural setting of a developing basin from seismic and potential-field data, in "Extensional Tectonics in the Basin and Range, the Aegean, and Western Anatolia," edited by Ibrahim Çemen, Elizabeth Catlos and Yildirim Dilek, Tectonophysics. doi:10.1016/j.tecto.2009.05.029.

Faulds, J.E., Henry, C.D., Hinz, N.H., 2005. Kinematics of the northern Walker Lane; an incipient transform along the Pacific–North American Plate boundary. Geology 33, 505–508.

Fosdick, J.C., Egger, A., Colgan, J.P., Surpless, B.E., Miller, E.L., Lerch, D.W., 2005. Cenozoic evolution of the northwestern boundary of the Basin and Range: geologic constraints from the Warner Range and Surprise Valley region. Geological Society of America, Abstracts with Programs 37 (7), 70.

Foster, A.N., Jackson, J.A., 1998. Source parameters of large African earthquakes; implications for crustal rheology and regional kinematics. Geophysical Journal International 134, 422–448.

Friedrich, A.M., Lee, J., Wernicke, B.P., Sieh, K., 2004. Geologic context of geodetic data across a Basin and Range normal fault, Crescent Valley, Nevada. Tectonics 23. doi:10.1029/2003TC001528.

Gans, P.B., Miller, E.L., McCarthy, J., Ouldcott, M.L., 1985. Tertiary extensional faulting and evolving ductile–brittle transition zones in the northern Snake Range and vicinity: new insights from seismic data. Geology 13, 189–193.

Please cite this article as: Lerch, D.W., et al., The northwestern margin of the Basin-and-Range Province, part 1: Reflection profiling of the moderate-angle (~30°) Surprise Valley Fault, Tectonophysics (2009), doi:10.1016/j.tecto.2009.05.028

Gashawbeza, E.M., Klemperer, S.L., Miller, E.L., Wilson, C.K., 2008. Nature of the crust beneath northwest Basin and Range province from teleseismic receiver function data. Journal of Geophysical Research 113, B10308. doi:10.1029/2007JB005306.

Goodliffe, A.M., Taylor, B., 2007. The boundary between continental rifting and sea-floor spreading in the Woodlark Basin, Papua New Guinea. In: Karner, G.D., Manatschal, G., Pinheiro, L.M. (Eds.), Imaging, Mapping and Modelling Continental Lithosphere Extension and Breakup. In: Special Publications, vol. 282. Geological Society, London, pp. 217–238.

Hammond, W.C., Thatcher, W., 2005. Northwest Basin and Range tectonic deformation observed with the Global Positioning System, 1999–2003. Journal of Geophysical Research 110 (B10). doi:10.1029/2005JB003678.

Hayward, N.J., Ebinger, C.J., 1996. Variations in the along-axis segmentation of the Afar Rift system. Tectonics 15, 244–257.

Hedel, C.W., 1984. Maps showing geomorphic and geologic evidence for late Quaternary displacement along the Surprise Valley and associated faults, Modoc County, California. U.S. Geological Survey Miscellaneous Field Studies Map, MF-1299.

Heiskanen, W.A., Vening Meinesz, F.A., 1958. The Earth and Its Gravity Field. McGraw-Hill Book Co., New York. 470 pp.

Johnson, R.A., Loy, K.L., 1992. Seismic reflection evidence for seismogenic low-angle faulting in southeastern Arizona. Geology 20, 597–600.

Kennedy, B.M., van Soest, M.C., 2006. A helium isotope perspective on the Dixie Valley, Nevada, hydrothermal system. Geothermics 35, 26–43.

Lerch, D.W., Klemperer, S.L., Glen, J.M.G., Ponce, D.A., Miller, E.L., Colgan, J.P., 2007. Crustal structure of the northwestern Basin and Range and its transition to unextended volcanic plateaus. Geochemistry, Geophysics, and Geosystems 8. doi:10.1029/2006GC001429, (Q02011).

Lerch, D.W., Klemperer, S.L., Stokoe, K.H., Menq, F.Y., 2008. Integration of the NEES T-Rex vibrator and PASSCAL Texan recorders for seismic profiling of shallow and deep crustal targets. Seismological Research Letters 79, 41–46.

McLeod, E.R., 1951. Hot spring erupts in farmer's meadow (California). Mineralogist 19, 431–433.

Miller, E.L., Colgan, J.P., Surpless, B.E., Riedel, S., Strickland, A., Egger, A.E., Benoit, D., 2005. Drill core data from the Warner Range and Surprise Valley. Geological Society of America, Abstracts with Programs 37 (7), 203–204.

Okaya, D.A., Thompson, G.A., 1985. Geometry of Cenozoic extensional faulting: Dixie Valley, Nevada. Tectonics 4, 107–125.

Oldow, J.S., 2003. Active transtensional boundary zone between the western Great Basin and Sierra Nevada block, western U.S. Cordillera. Geology 31, 1033–1036.

Personius, S.F., Mahan, S.A., 2005. Unusually low rates of slip on the Santa Rosa Range fault zone, northern Nevada. Bulletin of the Seismological Society of America 95, 319–333.

Personius, S.F., Crone, A.J., Machette, M.N., Lidke, D.J., Bradley, L.-A., and Mahan, S.A., (2007), Logs and scarp data from a paleoseismic investigation of the Surprise Valley fault zone, Modoc County, California: U.S. Geological Survey Scientific Investigations Map 2983, 2 sheets.

Proffett, J.M., 1977. Cenozoic geology of the Yerington District, Nevada, and the implications for the nature and origin of Basin and Range faulting. Geological Society of America Bulletin 88, 247–266.

Reheis, M.C., Sarna-Wojcicki, A.M., Reynolds, R.L., Repenning, C.A., Mifflin, M.D., 2002. Pliocene to middle Pleistocene lakes in the western Great Basin; ages and connections. In: Hershler, R., Madsen, D.B., Currey, D.R. (Eds.), Great Basin Aquatic Systems History. In: Smithsonian Contributions to the Earth Sciences, vol. 33. Smithsonian Institution, pp. 53–108.

Sachpazi, M., Clément, C., Laigle, M., Hirn, A., Roussos, N., 2003. Rift structure, evolution, and earthquakes in the Gulf of Corinth, from reflection seismic images. Earth and Planetary Science Letters 216, 243–257.

Slotnick, M.M., 1959. Lessons in Seismic Computing. Society of Exploration Geophysicists, Tulsa, OK. 268 pp.

Surpless, B.E., Stockli, D., Dumitru, T.A., Miller, E.L., 2002. Two-phase westward encroachment of Basin and Range extension into the northern Sierra Nevada. Tectonics 21 (1). doi:10.1029/2000TC001257.

Thompson, G.A., Meister, L.J., Herring, A.T., Smith, T.E., Burke, D.B., Kovach, R.L., Burford, R.O., Salehi, I.A., Wood, M.D., 1967. Geophysical study of Basin–Range structure, Dixie Valley region, Nevada, U.S. Air Force Cambridge Research Laboratories Scientific Report AFCRL-66-848. 244 pp.

Turcotte, D.L., Schubert, G., 1982. Geodynamics; Applications of Continuum Physics to Geological Problems. John Wiley and Sons, New York. 528 pp.

Twiss, R.J., Moores, E.M., 1992. Structural Geology. W.H. Freeman and Company, New York.

Yilmaz, O., 2001. Seismic data analysis: processing, inversion, and interpretation of seismic data. Investigations in Geophysics No. 10. Society of Exploration Geophysicists, Tulsa, Okla.

Please cite this article as: Lerch, D.W., et al., The northwestern margin of the Basin-and-Range Province, part 1: Reflection profiling of the moderate-angle (~30°) Surprise Valley Fault, Tectonophysics (2009), doi:10.1016/j.tecto.2009.05.028